Sustainable Cities and Society 113 (2024) 105661

Contents lists available at ScienceDirect

Sustainable Cities and Society

journal homepage: www.elsevier.com/locate/scs

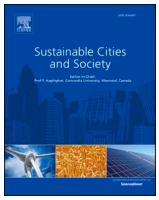

The potential of processed mineral construction and demolition waste to increase the water capacity of urban tree substrates - A pilot scale study in Munich

Sebastian Knoll [a,b], Simon Mindermann [c], Lauren Porter [d,e], Stephan Pauleit [f], Swantje Duthweiler [g], Johannes Prügl [a], Brigitte Helmreich [b,*]

[a] Bodeninstitut Johannes Prügl, Moosburger Str. 5, 84072 Au i. d. Hallertau, Germany
[b] Chair of Urban Water Systems Engineering, Technical University of Munich, Am Coulombwall 3, 85748 Garching, Germany
[c] Bavarian State Office for the Preservation of Monuments and Sites, Hofgraben 4, 80539 München, Germany
[d] Chair of Soil Science, School of Life Sciences, Technical University of Munich, Emil-Ramann-Str. 2, 85354 Freising, Germany
[e] TUM Working Group UPE Urban Productive Ecosystems, Hans-Carl-v.-Carlowitz-Platz 2, 85354 Freising, Germany
[f] Chair of Strategic Landscape Planning and Management, School of Life Sciences, Technical University of Munich, Emil-Ramann-Str. 6, 85354 Freising, Germany
[g] University of Applied Sciences Weihenstephan-Triesdorf, Am Staudengarten 7, 85354 Freising, Germany

ARTICLE INFO

Keywords:
Sustainable urban tree substrates
Waste recycling
Technosols
Constructed soils
Engineered soils
Purpose-designed soils

ABSTRACT

Construction and demolition waste (CDW) represents one of the most significant waste streams worldwide. Due to a high brick content, CDW amended soil substrates are expected to improve water retention, benefitting urban trees.

In this two-year field study evaluating the effects of CDW on the water holding capacities of urban tree substrates, six substrate mixtures are tested. Three test substrates contained a standard CDW mixture with 30 % and three 60 % bricks. Soil water contents were monitored and plant available water contents (PAWC) were analysed. From soil water contents and PAWC, the relative extractable water contents (REW), and subsequently the number of days with REW < 40 % and water stress intensity (WSI) are calculated.

The substrates with enhanced brick content showed higher PAWC. However, the effect of brick on PAWC was only significant at a minimum of 30 % bricks in the substrate. Pore size distribution of the brick fraction confirmed the assumed relationship between addition of brick and increased PAWC. Substrates with an enhanced brick content showed reduced numbers of days with REW < 40 % and a reduction in WSI.

Our findings demonstrate that CDW has potential to foster water holding capacities of urban tree substrates.

1. Introduction

The increase of urban tree cover is widely suggested as an important strategy for enhancing the resilience and adaptability of cities to climate change-related weather phenomena, (Erlwein & Pauleit, 2021; Fernandes et al., 2019; Hansen et al., 2022; Linke et al., 2022). Thanks to the provision of ecosystem services such as cooling effects and air cleaning, city trees lessen the adverse effects of climate change and improve environmental quality in urban areas (Pauleit et al., 2022; Rötzer et al., 2017;). However, the impacts of climate change in urban areas namely prolonged dry spells with increased temperatures threaten the vitality of urban trees (Marchin et al., 2022). Besides choosing drought-resistant species tree planting (Sjöman & Busse Nielsen, 2010; Sjöman et al., 2015), efforts must be increased to secure adequate root zones and increase soil substrates' ability to store stormwater for periods of drought (Caplan et al., 2019; Dervishi et al., 2022; Nielsen et al., 2007; Roloff et al., 2009; Stratópoulos et al., 2019; Zhang et al., 2020;).

Enhancing the pore volume of plant substrates is considered as a suitable measure to provide trees with sufficient amounts of water when root space is limited due to competition for space (FLL, 2010; Krieter & Malkus, 1996; Krieter et al., 1989). This is often achieved through porous primary or recycled soil additives. Recycled aggregates can help preserve natural resources, and their reuse is state-of-the-art in landscaping. For example, bottom ashes, shortfall batches of expanded clays, and pure, unblended brick aggregates are widely used in roof and tree substrates (City of Munich, 2018; FLL, 2018; Molineux et al., 2009,

* Corresponding author.
E-mail address: b.helmreich@tum.de (B. Helmreich).

https://doi.org/10.1016/j.scs.2024.105661
Received 14 February 2024; Received in revised form 10 July 2024; Accepted 10 July 2024
Available online 11 July 2024

2015; Roth-Kleyer, 2018; Schmilewsky, 2018). Recycled bricks enhance roadside trees and urban green substrates' vegetational and structural soil conditions (Bretzel et al., 2020; Willaredt & Nehls, 2021; Yilmaz et al., 20181;). Pure recycled brick aggregates from primary production waste are a permitted soil additive following the German fertilizer ordinance (German Federal Office of Justice, 2012). The possible application of impure brick material has been discussed in the context of ecological restoration (Bauer et al., 2022). Bauer et al. (2023) conducted a lab-scale study investigating the effects of brick substrates on growth of tree saplings. They suggested further research both for using larger plant spaces as well as the impact of re-used bricks from construction and building demolition wastes (CDW), which are mixed with concrete and mortar. In general, the recycling of bricks and concrete from CDW, which in many cases would otherwise only be disposed of in landfills, has a high potential to significantly contribute to reducing CO_2 emissions in the European Union (Caro et al., 2024). However, its potential to increase pore volumes in soils and their water storage capacity in tree planting sites are not well understood.

In this pilot scale study, we investigated the influence of CDW in different mixtures on plant-available water contents of urban tree substrates. Laboratory tests supplemented the field experiment. This study contributes to the recycling of CDW during the redevelopment of the 'Bayernkaserne' area in Munich, Germany, a former military compound into a new neighbourhood on an area of 48 ha. Demolition of existing buildings resulted in substantial amounts of CDW including not only building brick rubble but other components of construction, namely plaster, mortar, and concrete. This study aims to test urban tree substrates produced from CDW and residues and is focused on the following hypotheses:

1. Addition of CDW enhances the plant-available water of urban tree substrates, depending on brick ratios.
2. Higher brick ratios within CDW will allow a reduction in the number of days trees experience edaphic drought.

The study is paralleled by research on growth response and ecosystem services of the lime trees *Tilia cordata* planted, the results of which will be presented in a separate publication.

2. Material and methods

2.1. Study design

The processed CDW mixtures we used in this study originate from the demolition of old building stock at the 'Bayernkaserne' (Bayern barracks) in Munich, Germany (48° 11′ 58.0″ N; 11° 35′ 34.8″ E). After the buildings were cored, the building fabric was demolished: mostly brick structures with concrete elements, mortar joints and external plaster, but no wood or plastic. The demolition material was then crushed using a jaw crusher (e. g. Rubblemaster RM90), and steel reinforcements were removed using a magnetic separator. This processing of building debris resulted in two CDW recycling mixtures RCM relevant to this study: RCM1 and RCM2, both coming in fractions of 0–16 mm. Both RCM contain masonry bricks, mortar, concrete, and exterior plaster. Neither RCM1 nor RCM2 include any brick shingles.

RCM1 contains approx. 60 % bricks and 40 % concrete+mortar+plaster. This ratio is due to the proportion of masonry bricks, mortar in masonry joints, concrete elements and exterior plaster and results from manual re-sorting after the building demolition to increase the brick content and is the highest possible ratio of bricks in this study. RCM2 is designed to provide standard mixed recycled aggregates used in earthworks and road construction (FGSV, 2017, 2019, 2020). RCM2 contains approx. 30 % bricks and 70 % concrete+mortar+plaster.

The production of building bricks typically employs clays containing sand and lime (Benedix, 2020). Therefore, the mineralogical composition of brick fraction in CDW varies depending on parent material but usually is composed of quartz, clay minerals, feldspar, carbonates and iron-containing minerals, e. g. haematite, goethite, siderite, pyrite (Dunham, 1992, 2001). In the study area, concrete from CDW consists largely of calcite and dolomite (approx. 80 %) and quartz (Huber, 2021). The most critical components of the analysed CDW are likely to come from the mortar and plaster components that carry Portland cement. Portland cement consists largely of alite, belite, aluminate, and aluminate ferrite (Benedix, 2020). Therefore, the formation of new fracture surfaces during the crushing of the CDW can result in the formation of non-hydrated cement clinker phases, which can subsequently lead to secondary hydration processes and thus to the cementing of individual grains if there is sufficient contact with water (Dettenborn et al., 2014; Jitsangiam et al., 2014). Consequently, and in consideration potential increase in soil pH, EC and carbonate content, it can be argued that these CDW components in soil behave non-inert (Greinert & Kostecki, 2019, 2022).

Seven substrates were produced at the Bayernkaserne site (see Fig. 1).

In Germany, the guidelines of the German Landscape Development and Landscaping Research Society (Forschungsgesellschaft Landschaftsentwicklung Landschaftsbau e. V., FLL) are state of the art for tree planting in roadside greenery and are considered binding for public procurements (FLL, 2010). In Munich, the city's own regulations apply to public contracts (City of Munich, 2018). Both regulations define the vegetation properties of tree substrates. To ensure compliance with both regulations and to rule out overlapping effects on soil water content behaviour deriving from soil texture, structure, or soil organic matter content, soil physical properties were regulated accordingly and balanced by adding excavated and on-site processed topsoil (TS), subsoil (SS) as well as green waste compost (GWC). Mixing was carried out using a drum screen (Doppstadt SM518, mesh size = 32 mm) and, due to the coarse nature of Munich topsoil, all mixed substrates should have a grain size of 0–32 mm.

For this study, we designed and tested seven substrates:

1. group 'a' contains RCM1 in quantities of 75, 50 and 25 % CDW in the substrate (substrates *a1, a2, a3*),
2. group 'b' contains RCM2 in quantities of 75, 50 and 25 % CDW in the substrate (substrates *b1, b2, b3*),
3. one control substrate without any CDW, which is in accordance with the FLL guidelines for tree planting and the tree planting regulations of the City of Munich (substrate *fll*) (City of Munich, 2018; FLL, 2010).

Seven trial plots were constructed following the City of Munich's road construction and street tree planting guidelines (City of Munich, 2015, 2018). Each plot was appr. 4.0 m broad and appr. 30 m long. All substrates were backfilled and not compacted. After the material had settled, substrate layer depth in all plots was approx. 1.2 m. The plot's foundations were built from local unconsolidated bedrock. Low silt and clay contents characterize these quaternary gravels and have thus high permeability and negligible capillarity (Becher, 1970; Schick, 2002). Since the highest groundwater levels are expected to be at approx. 495 MASL (Dohr, 2022), and the bottom edges of the substrate layers are at ca. 498 MASL; we preclude both ground- and backwater influences on substrate water contents. Per row, we originally planted eight small-leaved lime trees *Tilia cordata 'Greenspire'* with trunk circumferences of 16 to 18 cm. The remaining surfaces had been evenly covered with turf (Fig. 2).

Irrigation was only carried out in the planting year 2020, after which precipitation and evapotranspiration regulated soil water contents exclusively.

2.2. Laboratory methods

Substrate and aggregate samples were tested in the laboratory of

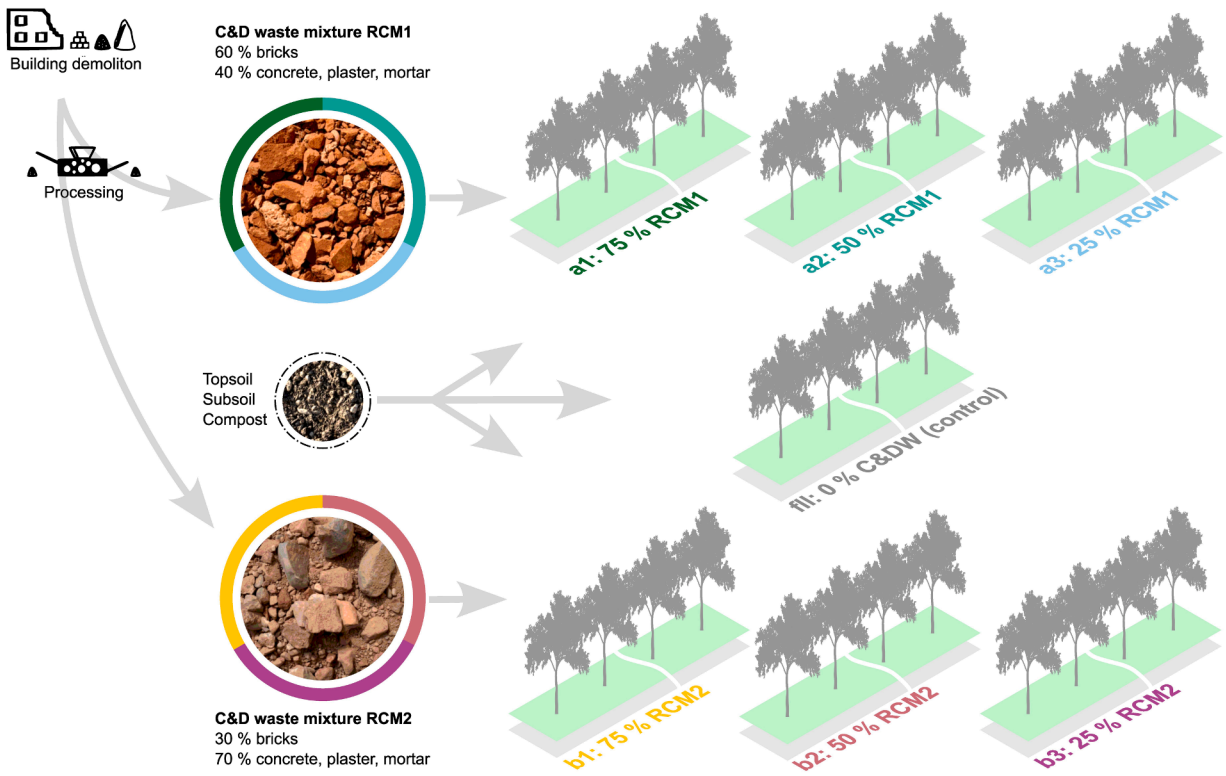

Fig. 1. Schematic illustration of the field experiment setup.

Fig. 2. *Left:* trial plots group *a* under construction, *right:* trial plots in summer 2023.

Bodeninstitut Prügl for physical properties. The substrate's pF values were acquired at the Chair of Soil Science, Technical University of Munich. The Scanning Electron Microsocpe SEM images of the brick fraction and the associated sample preparation were carried out at the scientific laboratory of the Bavarian State Office for the Preservation of Monuments and Sites.

2.2.1. Aggregate and substrate characteristics

Before installing the plots, CDW and substrates were sampled for a first assessment. To assess the percentages of raw brick material in the brick waste, single brick grains (grain diameters 4–16 mm) were separated manually from other mineral components (concrete+mortar+plaster) and quantified gravimetrically for fractions 4 to 8 mm and 8 to 16 mm after drying at 105 °C. Water absorptions of brick grains and concrete+mortar+plaster were measured according to the German Industry Norm DIN EN 1097-6:2022-05 (DIN, 2022). Grain size distributions of substrates were conducted according to DIN EN ISO 17, 892-4:2017-4 (DIN, 2009). Texture of the fine earth fraction was classified according to FAO guidelines for soil description (Jahn et al., 2006) and the German manual of soil mapping (Federal Institute for Geosciences & Natural Resources, 2005). Loss on ignition (LOI) of substrates were determined according to DIN EN 15,169:2007 (DIN, 2007). Infiltration rates were determined according to DIN 19,682-7 (DIN, 2015).

2.2.2. SEM image analysis of brick fraction

For SEM analysis, crushed brick samples were embedded in blue light hardening resin (Technovit 2000 LC, Kulzer GmbH) under vacuum, with the addition of an additive for polymerization inside the porosity (Technovit 2000 Inside Cure, Kulzer GmbH). The samples were manually ground, polished to a smooth surface, and sputter-coated with a gold-palladium alloy for conductivity. SEM images were produced with a Zeiss EVO 15 SEM (Carl Zeiss AG) at an acceleration voltage of 20 kV and an approximate working distance of 10 mm using a backscattered electron detector (BSE). Based on four SEM images with a magnification of 1,000x and a resolution of 278.64 × 208.98 µm and four SEM images with a magnification of 5,000x and a resolution of 56.26 × 42.2 µm pore size distributions were estimated by histogram-based thresholding followed by segmentation methods according to Buchner et al. (2021) using ImageJ software (Schneider et al., 2012). Mean total porosity and

mean pore area fractions were estimated by relating all pore areas of a specific pore range to the entire image area (supplementary information S1).

2.2.3. Soil water retention curves

For analyses of soil water retention curves (SWRCs), three undisturbed soil core samples per substrate were taken at a depth of 30 cm in Winter 2022/2023. SWRCs were determined using a suction plate (pore size 0.45 µm, EcoTech Umwelt-Messsysteme, Bonn, Germany) for pressures −10 hPa, −60 hPa and −300 hPa (corresponding to pF values of 1.0, 1.8 and 2.5 respectively) and using a pressure plate extractor (15 Bar Ceramic, Soilmoisture Equipment, Santa Barbara, California, USA) – for 2000 hPa and 15,000 hPa (pF 3.3 and 4.2 respectively). Plant available water contents (PAWC) [%] were calculated as the field capacity and wilting point differences. SWRCs were fitted according to Eq. (1):

$$\theta(h) = \theta_r + (\theta_s - \theta_r)S_e \quad (1)$$

where θ(h) is the volumetric water content at any given suction / pressure head, θ_r and θ_s are the residual and saturated water contents. $\theta_r = 0$ is a common assumption in bimodal models (Seki et al., 2022). Effective saturation S_e was calculated on basis of the multimodal dual-KO model (Seki et al., 2022; Seki et al., 2023) as Eq. (2):

$$S_e = w_1 Q\left[\frac{\ln(hh_{m1}^{-1})}{\sigma_1}\right] + (1 - w_1)Q\left[\frac{\ln(hh_{m2}^{-1})}{\sigma_2}\right] \quad (2)$$

Where Q (Eq. (3)):

$$Q(x) = \frac{erfc\left(\frac{x}{\sqrt{2}}\right)}{2} \quad (3)$$

and the values for w_1, σ, and h_m derived from the SWRC fit library (Seki, 2007). Standard errors of mean SE were calculated for every SWRC.

For the interpretation of SWRCs and SEM analyses, pore ranges were classified according to the German manual of soil mapping (Federal Institute for Geosciences & Natural Resources, 2005).

2.3. Field methods

2.3.1. Climate

Local meteorological data on precipitation (type 15,189, LAMBRECHT meteo GmbH, Göttingen, Germany), air temperature, and humidity (type c 2.3 KPC1/x, Galltec+mela, Bondorf, Germany) were collected on-site at intervals of 5 min. Because of a data gap from March to June 2022, the data for air temperature and humidity of Deutscher Wetterdienst (DWD) station 487, which was 5.5 km away, was used. For comparison, average air temperature and precipitation were calculated from 1991 to 2020 from HYRAS raster data sets. (DWD, 2022, 2023). Mean diurnal vapour pressure deficit VPD was calculated according to Zotarelli et al. (2010).

2.3.2. Soil volumetric water contents and relative extractable water

Soil volumetric water contents θ were measured in situ in depths of 25 cm, 50 cm, and 100 cm below ground in intervals of 10 min., using soil moisture sensors (type SMT 100, Truebner GmbH, Neustadt, Germany) connected to a data logger (UGT Umwelt-Geraete-Technik GmbH, Muencheberg, Germany). Each plot was equipped with three sensors per depth level. The capacitive sensor SMT 100 is based on the time domain transmission principle and measures soil apparent dielectric permittivity ε_a, which is correlated to soil moisture (Huebner, 2016; Truebner, 2022). According to the factory setting, ε_a would be converted to θ based on the widely used Topp equation (Topp et al., 1980). However, soil-specific calibration of the sensors is essential to prevent false interpretations due to the influence of texture, bulk density, salinity, and organic matter (Adla et al., 2020; Morgan et al., 1999; Starr & Paltineanu, 2002). We calibrated the sensor data using soil cylinders (d = 150 mm, V = 3000 cm^3), which were completely saturated with water and then successively dried while stepwise determination of ε_a and gravimetric water contents. The process was repeated three times. Calibration curves were developed for each substrate (supplementary information S2).

To identify drought stress, θ was converted to the relative extractable soil water content REW [%] according to Eq. (4):

$$REW\ [\%] = 100 * \left(\frac{\theta - \theta_{WP}}{PAWC}\right) \quad (4)$$

where θ is the actual θ at any given time, θ_{WP} is the substrate specific θ at wilting point and PAWC is the difference of field capacity θ_{FC} and wilting point θ_{WP} (Granier et al., 2007). Using the calculated diurnal REW, duration and intensity of periods of water scarcity were compared. The number of days on which the REW value dropped below a certain critical limit CL_{REW} were calculated for the 0–25 cm soil compartment and depth-weighted for the 0–100 cm soil compartment according to Eq. (5) (Puhlmann et al., 2019).

$$Days_{REW<CL}\ [d] = \sum_{i=begin\ veg.period}^{end\ veg.period} \begin{cases} REW_i < CL_{REW} : 1 \\ REW_i \geq CL_{REW} : 0 \end{cases} \quad (5)$$

The relative shortage of water volume when REW fell below a certain CL_{REW}, and thus the intensity of the water shortage, were calculated for the 0–25 cm soil compartment and depth-weighted for the 0–100 cm soil compartment from the value $Waterstress_{REW<40}$ according to Eq. (6) (Puhlmann et al., 2019).

$$Waterstress_{REW<CL}[\%] = \sum_{i=begin\ veg.period}^{end\ veg.period} \begin{cases} REW_i < CL_{REW} : 1 - \dfrac{REW_i}{CL_{REW}} \\ REW_i \geq CL_{REW} : 0 \end{cases} \quad (6)$$

For this study, CL_{REW} = 40 % is defined as the physiological threshold below which soil water becomes critical for plant transpiration due to stomatal closure (Granier et al., 1999).

2.4. Statistical methods

To find significant differences between the test substrates and the FLL control substrate for diurnal $Waterstress_{REW<40}$ in growing seasons 2022 and 2023, Kruskal-Wallis and Mann-Whitney U tests were conducted. Statistical analyses were conducted using Python packages NumPy (Harris et al., 2020), pandas (McKinney, 2010) statsmodels (Seabold & Perktold, 2010) and SciPy (Virtanen et al., 2020). Charts and diagrams were created using Python packages Matplotlib (Hunter, 2007) and seaborn (Waskom, 2021).

3. Results and discussion

3.1. Aggregate and substrate characteristics

RCM1 contains 60.7 % bricks and 39.3 % concrete+mortar+plaster in the fraction 4–16 mm. RCM2 contains 28.9 % bricks and 71.1 % concrete+mortar+plaster in fraction 4–16 mm. Brick ratios in the test substrate mixtures were in *a1, a2, a3* from 14 to 41 % and in *b1, b2*, and *b3* range from 20 to 41 %, respectively. Ratios of concrete+mortar+plaster range from 9 to 27 % for *a1, a2, a3*, and 16 to 48 % for *b1, b2*, and *b3* (cf. Table 1).

Water absorption of bricks in the fraction 4–16 mm was 14.9 ± 0.23 wt%, whereas water absorption of concrete+mortar+plaster in the fraction 4–16 mm was 2.04 ± 0.45 wt%.

Grain size distributions of the test and control substrates were similar (see supplementary information S3). Particle sizes < 0.063 mm ranged from 14.2 % (*b1*) to 16.1 % (*a1*). Sand contents (0.063–2 mm) range

Table 1
Composition and soil specific properties of all substrates investigated. CDW = construction & demolition waste, GWC = green waste compost, TS = topsoil, SS = subsoil, SL =Sandy loam according to FAO (Jahn et al., 2006), Sl4 = very loamy sand according to Federal Institute for Geosciences and Natural Resources (2005), LOI = loss on ignition, K = hydraulic conductivity.

Sample	CDW	Material ratios [% v/v]				Grain size distribution Size ranges [% w/w]			Texture of the fine earth fraction	Organic Matter content [% w/w]	Soil water characteristics [% v/v]			K [m/s] ± SD
		Bricks	Concrete + mortar + plaster	GWC	TS + SS	< 63 µm	63 µm – 2 mm	>2 mm	FAO / KA5	LOI ± SD	θ_{FC} ± SD	θ_{WP} ± SD	PAWC ± SE	
a1	RCM1: 75 %	41	27	10	22	16.1	28.0	55.9	SL / Sl4	2.95 ± 0.47	29.7 ± 2.1	5.6 ± 0.9	24.1 ± 0.3	$1.76\times10^{-3} \pm 1.7 \times 10^{-4}$
a2	RCM1: 50 %	28	18	10	44	15.1	30.3	54.6	SL / Sl4	2.68 ± 0.41	27.6 ± 1.5	6.9 ± 0.9	20.7 ± 0.3	$1.04\times10^{-3} \pm 7.6 \times 10^{-5}$
a3	RCM1: 25 %	14	9	10	67	15.1	30.6	54.3	SL / Sl4	2.48 ± 0.16	25.5 ± 1.7	7.2 ± 0.8	18.3 ± 0.2	$1.14\times10^{-3} \pm 8.1 \times 10^{-5}$
b1	RCM2: 75 %	20	48	10	22	14.2	28.0	57.8	SL / Sl4	2.08 ± 0.03	24.3 ± 1.9	5.7 ± 0.8	18.6 ± 0.3	$2.2 \times 10^{-4} \pm 1.4 \times 10^{-5}$
b2	RCM2: 50 %	14	32	10	44	14.3	27.1	58.5	SL / Sl4	2.89 ± 0.06	23.0 ± 1.9	6.8 ± 1.2	16.2 ± 0.3	$2.8 \times 10^{-4} \pm 1.6 \times 10^{-5}$
b3	RCM2: 25 %	7	16	10	67	15.4	30.2	54.4	SL / Sl4	2.92 ± 0.03	24.4 ± 1.0	7.2 ± 1.2	17.2 ± 0.3	$3.1 \times 10^{-4} \pm 1.7 \times 10^{-5}$
fll	–	–	–	10	90	14.3	30.2	55.5	SL / Sl4	2.76 ± 0.20	24.4 ± 0.8	7.7 ± 1.1	16.7 ± 0.3	$9.63\times10^{-4} \pm 5.6 \times 10^{-5}$

from 27.1 % (*b2*) to 30.6 % (*a3*). Gravel contents > 2 mm ranged from 54.6 % (*a2*) to 58.5 % (*b2*). Texture of the fine earth fraction of all substrates can be classified either as sandy loam (FAO) or very loamy sand (German manual for soil mapping), respectively. Loss on ignition LOI showed negligible differences and ranged from 2.08 ± 0.03 to 2.95 ± 0.47 %. Hydraulic conductivity was highest in group *a* and lowest in group *b* (see Table 1).

3.2. SEM image analysis of brick fraction

According to pore size distribution estimations by SEM image analyses, 0.4 % of pores were attributable to pores with an equivalent pore diameter of < 0.2 µm (beyond wilting point), 75.8 % to pores with an equal pore diameter of 0.2–3.0 µm, 22.6 % to pores with an equivalent pore diameter of 3.0–10.0 µm and 1.2 % to pores with an equivalent pore diameter of > 10 µm.

3.3. Soil water retention

θ_{FC} ranged from 23.0 to 29.7 %, and θ_{WP} ranged from 5.6 to 7.7 %, resulting in differences in PAWC, which was lowest in *b2* (16.2 % ± 0.3) and highest in *a1* (24.1 % ± 0.3). PAWC of *fll* was 16.7 ± 0.3. In group *a*, increasing PAWC was associated with increasing brick contents. PAWC in group *b* showed negligible differences compared to FLL substrates. While no significant differences in PAWC were found for substrates containing less than 30 % brick grains (*a3, b1, b2, b3*), PAWC was significantly increased in substrates *a1* and *a2* compared to *fll* (see Fig. 3). An increase of PAWC is correlated with increasing brick ratios in the substrates ($r^2 = 0.86$).

3.4. Field data

3.4.1. Climate

Spring 2022 started with relatively high precipitation in April and May. Summer 2022 was characterized by high temperatures, and in June and July 2022 precipitation was exceptionally low. Rainfall in

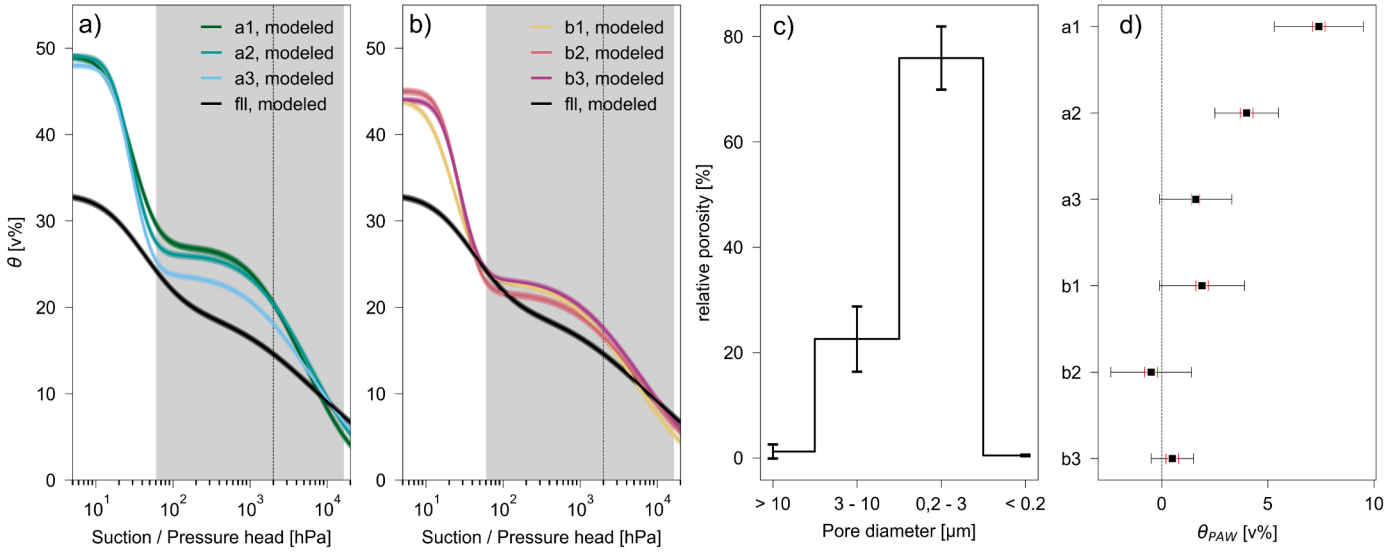

Fig. 3. a) and b) Soil water retention curves of groups a and b; grey areas mark plant available water contents, dotted lines mark the REW_{40} threshold at pF ≈ 3.3, c) porosity of brick fraction, d) mean differences of PAWC in comparison with the *fll* control substrate with SD (black error bars) and SE (red error bars).

August 2022 was higher than usual. Late summer was characterized by moderately high rainfall and high air temperature.

Spring 2023 started with relatively high precipitation in March and April, which proceeded to decline in May. In June and July 2023, precipitation was low. All summer, air temperature was higher than in the reference period. While precipitation in August 2023 was higher than usual, there was very little in September and October (see Fig. 4).

Both growing seasons were characterized by longer dry periods with higher temperatures, so we assume that roughly comparable climatic conditions prevailed in both growing seasons. The $Days_{REW<40}$ and $Waterstress_{REW<40}$ values discussed in the following chapter are, therefore, summarised and always refer to measured values from both growing seasons.

3.4.2. *Relative extractable soil water content and water stress intensity*

During the summer of 2022 and 2023, when both plant and atmospheric water demand were high and prolonged periods without precipitation dominated, REW values dropped considerably (Fig. 5). Differences were most pronounced in summer 2022, when REW in group 'a' was still moderate and mostly above REW_{40}. In summer 2023, REW at all depth levels fell below REW_{40} from June to mid-August. REW at depths of −100 cm is naturally the most insensitive and inertial to precipitation events. In the dry and hot summer of 2023, there was not even a significant effect of rain events on the REW at a depth of −50 cm. It can be observed that throughout all depth levels, group *a* tended to have higher REW than *fll*, while group *b* has consistently lower REW than *fll*.

Compared to *fll*, we found differences for days with REW < 40 % (Table 2). At depth level 0–25 cm, group *a* consistently had fewer and group *b* consistently more dry stress days. The most significant differences were found for *a1*, which had at least 77 fewer, and *b1*, which had at least 22 more water stress days. These trends were similar at depth level 0–100 cm, albeit less pronounced.

Compared to *fll*, we found no significant differences for water stress intensity during water stress days for group *a* at depth level 0–25 cm. In contrast, all substrates in group *b* had significantly higher water stress. In depth level 0–100, all substrates in group *a* had significantly less water stress intensity where all substrates in group *b* had significantly higher water stress intensity (Fig. 6).

4. Discussion

The water absorption tests of the brick material suggested that, in contrast to concrete+mortar+plaster, the brick fraction can potentially improve the water capacity of the tested substrates. The pore size distribution derived from the SEM image analysis shows, that most of the water absorbed in the pores of the brick fraction is plant-available. On the other hand, more than two thirds of the pore water appear to be stored in finer mesopores. This implies, that this pore water can be associated with plant water stress already. Higher porosities were reported for brick aggregates in technosols (Willaredt & Nehls, 2021). We assume recycled brick grains for commercial substrates are made from brick production waste. These modern masonry bricks can have significantly higher porosities (Buchner et al., 2021; Cultrone et al., 2004). As the material source in this study is old building stock from before the Second World War, these bricks generally have a lower porosity.

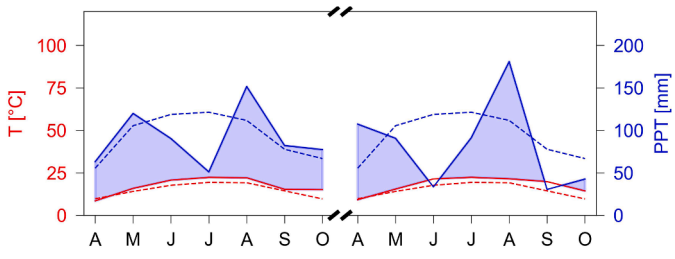

Fig. 4. The study site's Walter and Lieth climate diagram for vegetation periods 2022 and 2023. For comparison, dashed lines indicate long-term means for precipitation and air temperature (reference period: 1991 – 2020; (DWD, 2022, 2023)).

Soil properties such as organic matter content, soil texture, and porosity of aggregates contribute to differences in SWRCs (Bucka et al., 2019; Willaredt & Nehls, 2021). Of course, tree substrates according to FLL standard can cover a wide range of texture and organic matter (FLL, 2010; Schütt et al., 2022a). Since differences of LOI and grain size distributions of all substrates investigated are minor, soil organic matter and texture can be neglected as driving factors for differences in water capacity between the substrates tested in this study. Therefore, we conclude that differences in soil water retention are mainly due to the different proportions of bricks, which positively correlate with PAWC. Accordingly, the SWRC of group *a* show that the PAWC increases with an increasing proportion of RCM1 and a correspondingly increasing proportion of bricks. However, a significant effect is only seen from a brick content of at least 30 % (substrates *a1* and *a2*). This is confirmed by the results of group *b*, in which the substrates contained RCM2, which had no significant effect on PAWC, supposedly because none of the mixtures contained more than 30 % bricks. This may explain why Bauer et al. (2023) did find only marginal effects on tree saplings, as the substrates they tested did not contain more than 30 % brick aggregates. Bretzel et al. (2020), on the other hand, found significant differences for annual shoot growth – a proxy for annual drought stress (Liu et al., 2022) - of Linden trees planted in substrates which contained 85 % brick aggregates, but without any other CDW component.

In concordance with the pore distributions of brick fraction, the SWRC slopes of the substrates suggest that the addition of CDW causes multimodal pore distributions and, thus, a change in soil water retention and that the absorbed water can be partially extracted by plants only at higher suction tensions. We assume that this effect is negligible if, as with substrates *a1* and *a2*, the total PAWC is significantly increased. In contrast, for group *b* this would mean that the addition of RCM2 with the same PAWC as *fll* would increase the overall stress on trees.

These differences based on laboratory data are more pronounced in the field test. These differences are not significant for group *a* compared to *fll* at the 0–25 cm depth level, but they are significant for group *b*. At this depth level, meteorological phenomena have a greater effect on evaporation, as does the transpiration of the turf cover. We consider the 0–100 cm depth range to be more relevant for assessing water availability for tree roots. Here we see a decreasing edaphic drought stress with increasing proportions of RCM1. In contrast, an increasing proportion of RCM2 shows increasing edaphic drought stress, which was not expected from the laboratory tests. Our study cannot answer the question of why the drought stress measured in the field experiment is as high as it is in the substrates based on RCM2. We suspect that the CDW components of the concrete+plaster+mortar have a negative effect on water retention compared to a natural mineral matrix such as that in *fll*. Substrate *b1*, which contains approx. 50 % of concrete+plaster+mortar, also enters both growing seasons with already low water contents below field capacity. We have to hypothesize that the chemical properties of these materials make rewettability and corresponding water absorption more difficult during wet-dry cycles. Although both groups contain these components, water stress reduction through an increased brick content in Group *a* appear to compensate for or outweigh these adverse effects on water retention.

We can deduce two major limitations of our study: We cannot draw firm conclusions about the negative impact of the CDWs non-brick components on water stress intensities. In addition, this study is limited to two CDW mixtures of the same origin with a grain size of 0–16 mm. Therefore, future studies should investigate further CDW mixtures of different origins, grain sizes and ages, and consider the limitations imposed by the non-brick constituents of mineral CDW namely concrete, mortar and plaster. To gain a more comprehensive mechanistic

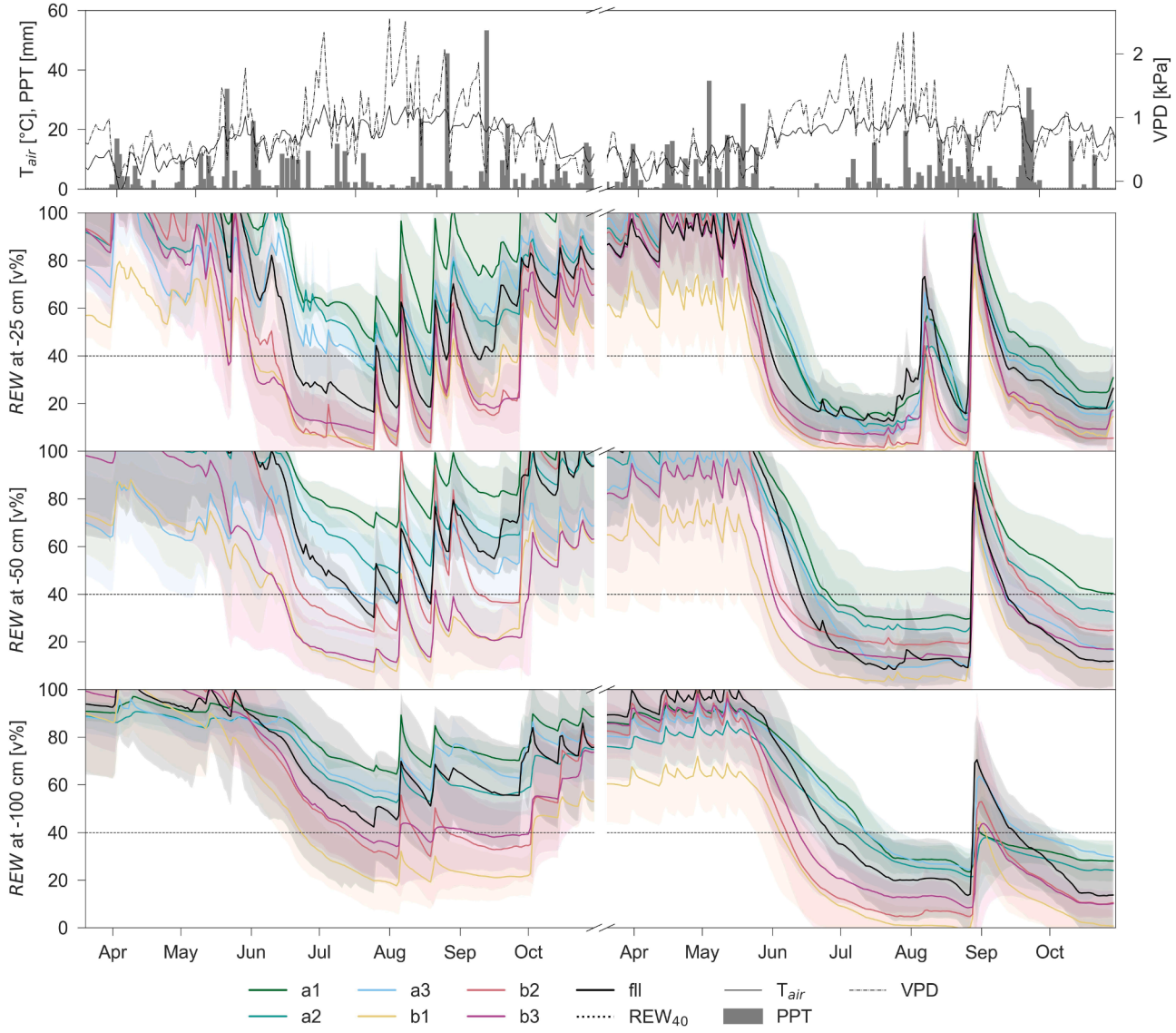

Fig. 5. REW for the depth levels −25 cm, −50 cm, and −100 cm during vegetation periods 2022 and 2023.

Table 2
Number of water stress days during both vegetation periods.

sample	$Days_{REW<40}$ [d] ± SD	
	0–25 cm	0–100 cm
a1	103 ± 32	91 ± 24
a2	132 ± 28	116 ± 17
a3	135 ± 18	119 ± 5
b1	265 ± 23	265 ± 13
b2	246 ± 26	222 ± 14
b3	252 ± 23	249 ± 31
fll	184 ± 36	159 ± 33

understanding, future studies should also focus on the water retention curves of substrates amended with CDW in repetitive wet-dry cycles. Due to the chemical (increase in alkalinity, electric conductivity and salinity, carbonates) and physical properties (e.g. subsequent cementation of soil and CDW particles) of CDW, long-term studies are necessary to investigate the effects on root and plant growth.

5. Conclusions

The addition of construction and demolition waste CDW to urban tree substrates can positively impact water holding capacities. The key findings of our two-year study evaluating the effects of CDW on water holding capacities of urban tree substrates are that CDW has the potential both to improve their plant available water contents and reduce water stress trough increased soil water contents during dry, hot periods. We found increases in PAWC to be dependant on the CDWs brick ratio. Other CDW components such as concrete, mortar and plaster did not contribute to increases of PAWC in our study. Therefore, hypothesis 1 can be accepted. Based on our results, a substantial improvement in PAWC of tree substrates can only be expected from brick contents of at least 30 %. However, the interpretations of this study are limited by the fact that the CDW grain size (0–16 mm) was comparatively coarse. We would expect that a finer grain size of CDW would provide more surface area for water to accumulate and contribute more to improving water retention. In addition, the brick aggregates in our study come from older bricks, which can be less porous than modern bricks.

In conclusion, under natural conditions during vegetation periods 2022 and 2023, the use of standard processed CDW for road construction and earthworks (RCM2) intensified edaphic drought compared to a

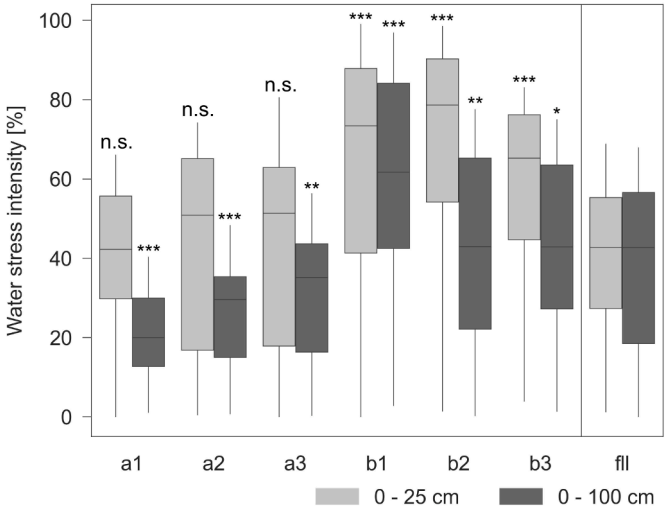

Fig. 6. Water stress intensity for vegetation periods 2022 and 2023 based on diurnal values for $Waterstress_{REW<40}$ for a) depth level 0–25 cm and b) depth level 0–100 cm. Mann-Whitney U p-value significance levels refer to the comparison with the *fll* control substrate: n.s.: $p > 0.05$; *: $p \leq 0.05$; **: $p \leq 0.01$; *** $p \leq 0.001$.

tree substrate according to the guidelines of the German Landscape Development and Landscaping Research Society (Forschungsgesellschaft Landschaftsentwicklung Landschaftsbau e. V., FLL) in our study. On the other hand, the field trial demonstrated that CDW, which has an increased brick content (RCM1) can significantly reduce both the number of water stress days and water stress intensity during dry and hot summer periods. Therefore, hypothesis 2 can be accepted.

These results suggest that in order to contribute to water storage in urban tree substrates, in addition to the mere disposal of CDW, a high proportion of bricks in the CDW must be ensured already during demolition by selective dismantling and before processing by further sorting steps. In the long term, and in comparison to conventional substrates, we expect the use of such quality-assured and locally recycled CDW as an aggregate for urban tree substrates to have an environmental impact by conserving natural resources. Furthermore, we anticipate reduced acquisition costs for urban tree substrates, reduced disposal costs for construction and demolition waste, and a reduction in related CO_2 emissions. These factors collectively contribute to a sustainable, cost-effective urban circular economy. The results from our field study emphasise the need to adapt urban tree substrates to the consequences of global warming if the irrigation requirements for urban tree populations are not to increase drastically (Dervishi et al., 2023; Schütt et al., 2022a; Schütt et al., 2022b). We therefore assume that in the future, the use of water-retaining agents as additives for substrates will become increasingly prevalent. The use of mineral construction and demolition waste as a structural material for urban tree substrates can help to increase plant available water in urban tree pits and alleviate edaphic drought in an economic and resource-friendly manor. We anticipate that the enhanced water absorption will reduce irrigation requirements and contribute to tree health and resilience in urban areas. Our results can be extrapolated to all urban areas that are already affected by prolonged droughts and high temperatures due to climate change and are likely to be in the future.

Nevertheless, the limitations of our study must be acknowledged. Future studies must address the long-term effects of the physical and chemical properties of mineral CDW on the growth of below- and aboveground biomass of trees in urban tree substrates, as well as its impact on their ecosystem services.

Funding

This research was funded by the City of Munich Municipal Department and contributed to the EU URBACT project URGE (circular building cities).

CRediT authorship contribution statement

Sebastian Knoll: Writing – original draft, Visualization, Validation, Methodology, Investigation, Funding acquisition, Formal analysis, Data curation, Conceptualization. **Simon Mindermann:** Writing – review & editing, Resources, Methodology. **Lauren Porter:** Writing – review & editing, Resources, Methodology. **Stephan Pauleit:** Writing – review & editing, Supervision, Conceptualization. **Swantje Duthweiler:** Conceptualization. **Johannes Prügl:** Supervision, Methodology, Funding acquisition, Conceptualization. **Brigitte Helmreich:** Writing – review & editing, Supervision.

Declaration of competing interest

The authors declare that they have no known competing financial interests or personal relationships that could have appeared to influence the work reported in this paper.

Data availability

Data will be made available on request.

Acknowledgements

The authors gratefully acknowledge the funding municipality the City of Munich that supported the study by funding and making areas for the field trial available. The authors thank Dr. Michael Beck for substantial technical advice concerning the measuring instruments. The authors thank Anton Knoll for contributing substantially to the electronic data acquisition setup as part of the field trial. The authors thank Dr. Franziska Bucka and Dr. Julien Guigue for their support during pF measurements at the chair of soil science, TU Munich.

Supplementary materials

Supplementary material associated with this article can be found, in the online version, at doi:10.1016/j.scs.2024.105661.

References

Adla, S., Rai, N., Karumanchi, H., Tripathi, S., Disse, M., & Pande, S. (2020). Laboratory calibration and performance evaluation of low-cost capacitive and very low-cost resistive soil moisture sensors. *Sensors, 20*, 363. https://doi.org/10.3390/s20020363

Bauer, M., Krause, M., Heizinger, V., & Kollmann, J. (2022). Using crushed waste bricks for urban greening with contrasting grassland mixtures: No negative effects of brick-augmented substrates varying in soil type, moisture and acid pre-treatment. *Urban Ecosystems*. https://doi.org/10.1007/s11252-022-01230-x

Bauer, M., Krause, M., Heizinger, V., & Kollmann, J. (2023). Increased brick ratio in urban substrates has a marginal effect on tree saplings. *Trees, 37*(3), 875–889. https://doi.org/10.1007/s00468-023-02391-8

Becher, H. H. (1970). *Eine methode zur messung der wasserleitfähigkeit im ungesättigten zustand*. Hannover.

Benedix, R. (2020). *Bauchemie* (7 ed.). Springer Vieweg.

Bretzel, F., Vannucchi, F., Pini, R., Scatena, M., Marradi, A., & Cinelli, F. (2020). Use of coarse substrate to increase the rate of water infiltration and the bearing capacity in tree plantings. *Ecological Engineering, 148*, Article 105798. https://doi.org/10.1016/j.ecoleng.2020.105798

Buchner, T., Kiefer, T., Zelaya-Lainez, L., Gaggl, W., Konegger, T., & Füssl, J. (2021). A multi technique, quantitative characterization of the pore space of fired bricks made of five clayey raw materials used in European brick industry. *Applied Clay Science, 200*, Article 105884. https://doi.org/10.1016/j.clay.2020.105884

Bucka, F. B., Kölbl, A., Uteau, D., Peth, S., & Kögel-Knabner, I. (2019). Organic matter input determines structure development and aggregate formation in artificial soils. *Geoderma, 354*, Article 113881. https://doi.org/10.1016/j.geoderma.2019.113881

Caplan, J., Galanti, R., Olshevski, S., & Eisenman, S. (2019). Water relations of street trees in green infrastructure tree trench systems. Urban For. *Urban Green, 41*, 170–178.
Caro, D., Lodato, C., Damgaard, A., Cristóbal, J., Foster, G., Flachenecker, F., & Tonini, D. (2024). Environmental and socio-economic effects of construction and demolition waste recycling in the European Union. *Science of The Total Environment, 908*, Article 168295. https://doi.org/10.1016/j.scitotenv.2023.168295
City of Munichs ZTV Stra-Mü (2015).: Zusätzliche Technische Vorschriften und Richtlinien für die Ausführung von Straßenbauarbeiten in München, (2015).
City of Munichs ZTV Vegtra-Mü (2018).: Zusätzliche Technische Vorschriften für die Herstellung und Anwendung verbesserter Vegetationstragschichten, (2018).
Cultrone, G., Sebastián, E., Elert, K., de la Torre, M. J., Cazalla, O., & Rodriguez–Navarro, C. (2004). Influence of mineralogy and firing temperature on the porosity of bricks. *Journal of the European Ceramic Society, 24*(3), 547–564. https://doi.org/10.1016/S0955-2219(03)00249-8
Dervishi, V., Fleckenstein, C., Rahman, M. A., Pauleit, S., Ludwig, F., Pretzsch, H., & Rötzer, T. (2023). Trees in planters – Growth, structure and ecosystem services of Platanus x hispanica and Tilia cordata and their reaction to soil drought. *Urban Forestry & Urban Greening, 86*, Article 128024. https://doi.org/10.1016/j.ufug.2023.128024
Dervishi, V., Poschenrieder, W., Rötzer, T., Moser-Reischl, A., & Pretzsch, H. (2022). Effects of climate and drought on stem diameter growth of urban tree species. *Forests, 13*, 641. https://doi.org/10.3390/f13050641
Dettenborn, T., Forsman, J., & Korkiala-Tanttu, L. (2014). Long-term behavior of crushed concrete in road structure.
DIN 19682-7 2015-08: Soil quality - Field tests - Part 7: Determination of infiltration rate by double ring infiltrometer, (2015).
DIN. (2007). DIN EN 15169:2007-05: Characterization of waste - Determination of loss on ignition in waste, sludge and sediments; German version EN 15169:2007. In (Vol. DIN EN 15169-05, pp. 16).
DIN. (2009). DIN EN ISO 17892-4:2017-4: Geotechnical investigation and testing - Laboratory testing of soil - Part 4: Determination of particle size distribution (ISO 17892-4:2016); German version EN ISO 17892-4:2016. In (Vol. DIN 19528, pp. 24).
DIN. (2022). DIN EN 1097-6:2022-05: Tests for mechanical and physical properties of aggregates - Part 6: Determination of particle density and water absorption; German version EN 1097-6:2022. In (Vol. DIN EN 1097–1096).
Dohr, V. (2022). *Grundwassersituation im oberen Grundwasserstockwerk - Isohypsen* 1990. Retrieved 18.08.2022 from https://geoportal.muenchen.de/portal/umwelt/?layerIDs=gsm:G_stadtkarte_gesamt,rgu:ISohypse_tiefbau,rgu:ISohypse_absenk,rgu:ISohypse_hw90_text,rgu:ISohypse_hw90_gw,rgu:ISohypse_hw90,rgu:ISohypse_fliess_90,rgu:ISohypse_mergel_90,rgu:ISohypse_morph,rgu:ISohypse_u_bahn,rgu:ISohypse_drainage&visibility=true,true,true,true,true,true,true,true,true,true,true,true&transparency=0,0,0,0,0,0,0,0,0,0,0&center=692883.9594410365,5339790.511374331&zoomlevel=4.
Dunham, A. C. (1992). Developments in industrial mineralogy: I. The mineralogy of brick-making. *Proceedings of the Yorkshire Geological Society, 49*(2), 95–104. https://doi.org/10.1144/pygs.49.2.95
Dunham, A. C., McKnight, A., & Warren, I. (2001). Mineral assemblages formed in oxford clay fired under different time–temperature conditions with reference to brick manufacture. In *, 53. Proceedings of The Yorkshire Geological Society - PROC YORKS GEOL SOC* (pp. 221–230). https://doi.org/10.1144/pygs.53.3.221
DWD. (2022). *Raster data set of daily mean temperature in °C for Germany - HYRAS-DE-TAS, Version v5.0*. https://opendata.dwd.de/climate_environment/CDC/grids_germany/daily/hyras_de/air_temperature_mean/.
DWD. (2023). *Raster data set of daily sums of precipitation in mm for Germany - HYRAS-DE-PRE, Version v3.0*. https://opendata.dwd.de/climate_environment/CDC/grids_germany/daily/hyras_de/precipitation/.
Erlwein, S., & Pauleit, S. (2021). Trade-offs between urban green space and densification: balancing outdoor thermal comfort, mobility, and housing demand. *Urban Planning, 6*. https://doi.org/10.17645/up.v6i1.3481
Federal Institute for Geosciences and Natural Resources. (2005). *Manual of soil mapping* (5th Ed.,, *5*. Bundesanstalt für Geowissenschaften und Rohstoffe *(KA5)*.
Fernandes, C. O., da Silva, I. M., Teixeira, C. P., & Costa, L. (2019). Between tree lovers and tree haters. Drivers of public perception regarding street trees and its implications on the urban green infrastructure planning. *Urban Forestry & Urban Greening, 37*, 97–108. https://doi.org/10.1016/j.ufug.2018.03.014
FGSV M RC (2019).: Merkblatt über den Einsatz von rezyklierten Baustoffen im Erd- und Straßenbau, (2019).
FGSV TL BuB E-StB (2020).: Technische Lieferbedingungen für Bodenmaterialien und Baustoffe für den Erdbau im Straßenbau, (2020).
FGSV ZTV E-StB (2017).: Zusätzliche Technische Vertragsbedingungen und Richtlinien für Erdarbeiten im Straßenbau, § 119 (2017).
FLL Empfehlungen für Baumpflanzungen – Teil 2. (2010). *Standortvorbereitungen für neupflanzungen; pflanzgruben und wurzelraumerweiterung, 66*. Bauweisen und Substrate.
FLL Green Roof Guidelines - guidelines for the planning, construction and maintenance of green roofs, 158 (2018).
German Federal Office of Justice. (2012). Verordnung über das Inverkehrbringen von Düngemitteln, Bodenhilfsstoffen, Kultursubstraten und Pflanzenhilfsmitteln (Düngemittelverordnung DüMV). *Bundesgesetzblatt Jahrgang, 2012*. Teil I Nr. 58. In. Bonn.
Granier, A., Bréda, N., Biron, P., & Villette, S. (1999). A lumped water balance model to evaluate duration and intensity of drought constraints in forest stands. *Ecological Modelling, 116*(2), 269–283. https://doi.org/10.1016/S0304-3800(98)00205-1
Granier, A., Reichstein, M., Bréda, N., Janssens, I. A., Falge, E., Ciais, P., Grünwald, T., Aubinet, M., Berbigier, P., Bernhofer, C., Buchmann, N., Facini, O., Grassi, G., Heinesch, B., Ilvesniemi, H., Keronen, P., Knohl, A., Köstner, B., Lagergren, F., … Wang, Q. (2007). Evidence for soil water control on carbon and water dynamics in European forests during the extremely dry year: 2003. *Agricultural and Forest Meteorology, 143*(1), 123–145. https://doi.org/10.1016/j.agrformet.2006.12.004
Greinert, A., & Kostecki, J. (2019). *Anthropogenic materials as bedrock of urban technosols*, 2019//. UrbanizationCham: Challenge and Opportunity for Soil Functions and Ecosystem Services.
Greinert, A., & Kostecki, J. (2022). Construction and demolition waste as a non-inert technogenic soil parent material. *SUITMA, 11*. online.
Hansen, R., Buizer, M., Buijs, A., Pauleit, S., Mattijssen, T., Fors, H., van der Jagt, A., Kabisch, N., Cook, M., Delshammar, T., Randrup, T., Erlwein, S., Vierikko, K., Nieminen, H., Langemeyer, J., Texereau, C., Luz, A., Nastran, M., Olafsson, A., & Konijnendijk, C. (2022). Transformative or piecemeal? Changes in green space planning and governance in eleven European cities. *European Planning Studies*. https://doi.org/10.1080/09654313.2022.2139594
Harris, C. R., Millman, K. J., van der Walt, S. J., Gommers, R., Virtanen, P., Cournapeau, D., Wieser, E., Taylor, J., Berg, S., Smith, N. J., Kern, R., Picus, M., Hoyer, S., van Kerkwijk, M. H., Brett, M., Haldane, A., del Río, J. F., Wiebe, M., Peterson, P., … Oliphant, T. E. (2020). Array programming with NumPy. *Nature, 585*(7825), 357–362. https://doi.org/10.1038/s41586-020-2649-2
Huber, S. (2021). *Ein beitrag zur bodenmechanischen und erdbautechnischen charakterisierung von recycling-baustoffen [Dissertation*. Munich: Technical University of Munich].
Huebner, C. K., & Udo. (2016). *Electromagnetic moisture measurement : Principles and applications*. Universitätsverlag Göttingen.
Hunter, J. D. (2007). Matplotlib: A 2D graphics environment. *Computing in Science & Engineering, 9*(3), 90–95. https://doi.org/10.1109/MCSE.2007.55
Jahn, R., Blume, H. P., Asio, V., Spaargaren, O., & Schad, P. (2006). *FAO guidelines for soil description*. Rome.
Jitsangiam, P., Boonserm, K., Phenrat, T., Chummuneerat, S., Chindaprasirt, P., & Nikraz, H. (2014). Recycled concrete aggregates in roadways: laboratory examination of self-cementing characteristics. *Journal of Materials in Civil Engineering, 27*, Article 04014270. https://doi.org/10.1061/(ASCE)MT.1943-5533.0001245
Krieter, M., Bill, A., Malkus, A., & Würding, G. (1989). *Standortoptimierung von straßenbäumen*. FLL-Arbeitskreis Straßenbäume. Issue. F. L. Landschaftsbau.
Krieter, M., & Malkus, A. (1996). *Untersuchungen zur Standortoptimierung von Straßenbäumen : Ergebnisse eines FLL-Pflanzversuches von tilia pallida in 14 deutschen Städten* (1 ed.). *Forschungsgesellschaft landschaftsentwicklung*. Landschaftsbau e.V., FLL.
Linke, S., Erlwein, S., van Lierop, M., Fakirova, E., Pauleit, S., & Lang, W. (2022). Climate change adaption between governance and government—collaborative arrangements in the city of Munich. *Land, 11*, 1818. https://doi.org/10.3390/land11101818
Liu, M., Pietzarka, U., Meyer, M., Kniesel, B., & Roloff, A. (2022). Annual shoot length of temperate broadleaf species responses to drought. *Urban Forestry and Urban Greening, 73*, Article 127592. https://doi.org/10.1016/j.ufug.2022.127592. Article.
Marchin, R. M., Esperon-Rodriguez, M., Tjoelker, M. G., & Ellsworth, D. S. (2022). Crown dieback and mortality of urban trees linked to heatwaves during extreme drought. *Science of The Total Environment, 850*, Article 157915. https://doi.org/10.1016/j.scitotenv.2022.157915
McKinney, W. (2010). Data structures for statistical computing in python. *Proceedings of the 9th Python in Science Conference, 445*, 51–56.
Molineux, C. J., Fentiman, C. H., & Gange, A. C. (2009). Characterising alternative recycled waste materials for use as green roof growing media in the U.K. *Ecological Engineering, 35*(10), 1507–1513. https://doi.org/10.1016/j.ecoleng.2009.06.010
Molineux, C. J., Gange, A. C., Connop, S. P., & Newport, D. J. (2015). Using recycled aggregates in green roof substrates for plant diversity. *Ecological Engineering, 82*, 596–604. https://doi.org/10.1016/j.ecoleng.2015.05.036
Morgan, K. T., Parsons, L. R., Wheaton, T. A., Pitts, D. J., & Obreza, T. A. (1999). Field calibration of a capacitance water content probe in fine sand soils. *Soil Science Society of America Journal, 63*(4), 987–989. https://doi.org/10.2136/sssaj1999.634987x
Nielsen, C. N., Buhler, O., & Kristoffersen, P. (2007). Soll water dynamics and growth of street and park trees. *Arboriculture and Urban Forestry, 33*(4), 231.
Pauleit, S., Gulsrud, N., Raum, S., Taubenböck, H., Leichtle, T., Erlwein, S., Rötzer, T., Rahman, M., & Moser-Reischl, A. (2022). *Smart Urban Forestry: Is It the Future?*, 161–182. https://doi.org/10.1007/978-3-031-03803-7_10
Puhlmann, H., Schmidt-Walter, P., Hartmann, P., Meesenburg, H., & von Wilpert, K. (2019). Soil water budget and drought stress. In N. Wellbrock, & A. Bolte (Eds.), *Status and dynamics of forests in germany : Results of the national forest monitoring* (pp. 55–91). Springer International Publishing. https://doi.org/10.1007/978-3-030-15734-0_3.
Roloff, A., Korn, S., & Gillner, S. (2009). The climate-species-matrix to select tree species for urban habitats considering climate change. *Urban Forestry & Urban Greening, 8*(4), 295–308. https://doi.org/10.1016/j.ufug.2009.08.002
Roth-Kleyer, S. (2018). Recyclingziegel für Vegetationssubstrate im GaLaBau. In *Neue landschaft, 8. 2/2018*.
Rötzer, T., Moser-Reischl, A., Pauleit, S., & Pretzsch, H. (2017). *Wachstum und Ökosystemleistungen von Stadtbäumen im Klimawandel*.
Schick, P. (2002). Anwendung eines Zwei-Komponenten-Modells der pF-Kurve auf Strukturänderungen in Böden. *Bautechnik, 79*(2), 13.
Schmilewsky, G. K. (2018). Kultursubstrate und Blumenerden - Eigenschaften. In *Ausgangsstoffe, verwendung, 1*. Industrieverband Garten e. V.
Schneider, C. A., Rasband, W. S., & Eliceiri, K. W. (2012). NIH Image to ImageJ: 25 years of image analysis. *Nature Methods, 9*(7), 671–675. https://doi.org/10.1038/nmeth.2089

Schütt, A., Becker, J. N., Gröngröft, A., Schaaf-Titel, S., & Eschenbach, A. (2022b). Soil water stress at young urban street-tree sites in response to meteorology and site parameters. *Urban Forestry & Urban Greening, 75*, Article 127692. https://doi.org/10.1016/j.ufug.2022.127692

Schütt, A., Becker, J., Reisdorff, C., & Eschenbach, A. (2022a). Growth response of nine tree species to water supply in planting soils representative for urban street tree sites. *Forests, 13*(6). https://doi.org/10.3390/f13060936. https://www.mdpi.com/1999-4907/1913/1996/1936/htm

Seabold, S., & Perktold, J. (2010). statsmodels: Econometric and statistical modeling with python. In *9th Python in Science Conference*.

Seki, K. (2007). SWRC Fit – A nonlinear fitting program with a water retention curve for soils having unimodal and bimodal pore structure. *Hydrology and Earth System Sciences Discussions*. https://doi.org/10.5194/hessd-4-407-2007

Seki, K., Toride, N., & Genuchten, M. T. V. (2023). Evaluation of a general model for multimodal unsaturated soil hydraulic properties. *Journal of Hydrology and Hydromechanics, 71*(1), 22–34. https://doi.org/10.2478/johh-2022-0039

Seki, K., Toride, N., & Th. van Genuchten, M. (2022). Closed-form hydraulic conductivity equations for multimodal unsaturated soil hydraulic properties. *Vadose Zone Journal, 21*(1), e20168. https://doi.org/10.1002/vzj2.20168

Sjöman, H., & Busse Nielsen, A. (2010). Selecting trees for urban paved sites in Scandinavia – A review of information on stress tolerance and its relation to the requirements of tree planners. *Urban Forestry & Urban Greening, 9*(4), 281–293. https://doi.org/10.1016/j.ufug.2010.04.001

Sjöman, H., Hirons, A. D., & Bassuk, N. L. (2015). Urban forest resilience through tree selection—Variation in drought tolerance in Acer. *Urban Forestry & Urban Greening, 14*(4), 858–865. https://doi.org/10.1016/j.ufug.2015.08.004

Starr, J. L., & Paltineanu, I. (2002). Methods for measurement of soil water content: Capacitance devices. *Methods of soil analysis: Part 4 physical methods* (pp. 463–474).

Stratópoulos, L., Zhang, C., Häberle, K.-H., Pauleit, S., Duthweiler, P., & Rötzer, T. (2019). Effects of drought on the phenology, growth, and morphological development of three urban tree species and cultivars. *Sustainability, 11*, 5117. https://doi.org/10.3390/su11185117

Topp, G. C., Davis, J. L., & Annan, A. P. (1980). Electromagnetic determination of soil water content: Measurement in coaxial transmission lines. *Water Resources Research, 16*(3), 574–582.

Truebner (2022). Soil moisture sensor SMT100, last request: 17.08.2022. In.

Virtanen, P., Gommers, R., Oliphant, T. E., Haberland, M., Reddy, T., Cournapeau, D., Burovski, E., Peterson, P., Weckesser, W., Bright, J., van der Walt, S. J., Brett, M., Wilson, J., Millman, K. J., Mayorov, N., Nelson, A. R. J., Jones, E., Kern, R., Larson, E., … SciPy, C. (2020). SciPy 1.0: Fundamental algorithms for scientific computing in Python. *Nature Methods, 17*(3), 261–272. https://doi.org/10.1038/s41592-019-0686-2

Waskom, M. L. (2021). Seaborn: Statistical data visualization. *Journal of Open Source Software, 9*. https://doi.org/10.21105/joss.03021

Willaredt, M., & Nehls, T. (2021). Investigation of water retention functions of artificial soil-like substrates for a range of mixing ratios of two components. *Journal of Soils and Sediments, 21*(5), 2118–2129. https://doi.org/10.1007/s11368-020-02727-8

Yilmaz, D., Cannavo, P., Séré, G., Vidal-Beaudet, L., Legret, M., Damas, O., & Peyneau, P.-E. (2018). Physical properties of structural soils containing waste materials to achieve urban greening. *Journal of Soils and Sediments, 18*(2), 442–455. https://doi.org/10.1007/s11368-016-1524-0

Zhang, C., Stratópoulos, L., Xu, C., Pretzsch, & Rötzer, T. (2020). Development of fine root biomass of two contrasting urban tree cultivars in response to drought stress. *Forests, 108*, 11. https://doi.org/10.3390/f11010108

Zotarelli, L., Dukes, M. D., Romero, C. C., Migliaccio, K. W., & Morgan, K. T. (2010). *Step by step calculation of the penman-monteith evapotranspiration (FAO-56 method)*. Doc. AE459, University of Florida. https://edis.ifas.ufl.edu/pdffiles/AE/AE45900.pdf.